

Cite this: *Chem. Sci.*, 2017, 8, 5797

Efficient photocatalytic carbon monoxide production from ammonia and carbon dioxide by the aid of artificial photosynthesis†

Zeai Huang,^a Kentaro Teramura,^{a,b} Hiroyuki Asakura,^{a,b} Saburo Hosokawa^{a,b} and Tsunehiro Tanaka^{a,b}

Ammonium bicarbonate (NH_4HCO_3) was generated by the absorption of carbon dioxide (CO_2) into an aqueous solution of ammonia (NH_3). NH_4HCO_3 was successfully used to achieve highly efficient photocatalytic conversion of CO_2 to carbon monoxide (CO). NH_3 and/or ammonium ions (NH_4^+) derived from NH_4HCO_3 in aqueous solution were decomposed into nitrogen (N_2) and hydrogen (H_2). Stoichiometric amounts of the N_2 oxidation product and the CO and H_2 reduction products were generated when the photocatalytic reaction was carried out in aqueous NH_4HCO_3 solution. NH_3 and/or NH_4^+ functioned as electron donors in the photocatalytic conversion of CO_2 to CO . A CO formation rate of 0.5 mmol h^{-1} was obtained using 500 mg of catalyst (approximately 7500 ppm) in ambient conditions (303 K, 101.3 kPa). Our results demonstrated that NH_4HCO_3 is a novel inorganic sacrificial reagent, which can be used to increase the efficiency of photocatalytic CO production to achieve one step CO_2 capture, storage and conversion.

Received 26th April 2017

Accepted 19th June 2017

DOI: 10.1039/c7sc01851g

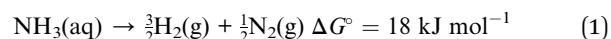
rsc.li/chemical-science

Introduction

The production of chemical feedstocks and hydrocarbon fuels from CO_2 is a promising approach to alleviate the global energy crisis and global warming.¹ Conversion of CO_2 to CO using clean and renewable solar energy is the first step to store energy in chemicals because CO can be further converted into other highly valuable chemicals using the Fischer–Tropsch process.² A variety of heterogeneous and homogeneous photocatalysts have been reported to achieve the conversion of CO_2 to CO .^{3–5} However, the formation rate of CO has been limited to a few tens of $\mu\text{mol h}^{-1}$ or hundreds of $\mu\text{mol h}^{-1} \text{ g}^{-1}$ because of the high energy barrier to CO_2 reduction and inefficient light utilization.^{6,7} Furthermore, CO_2 is not easily adsorbed onto catalytic surfaces nor activated by photoirradiation because of its high thermodynamic stability. This further reduces the efficiency of the photocatalytic conversion of CO_2 .

Water (H_2O) is widely used as an electron donor in the photocatalytic conversion of CO_2 to CO .^{7–12} However, the overall water splitting into H_2 and O_2 is more thermodynamically favorable than the reduction of CO_2 in aqueous solution. Hence,

CO_2 reduction competes with overall water splitting. Moreover, the solubility of CO_2 in pure H_2O is only 0.033 mol L^{-1} (at 298 K and 101.3 kPa),¹³ which further limits the efficiency of CO_2 conversion by H_2O using heterogeneous photocatalysts. Therefore, it would be meaningful to find a readily available, highly efficient, and abundant in nature and industries electron donor (sacrificial reagent) other than water for the photocatalytic conversion of CO_2 . NH_3 and NH_4^+ in aqueous solution can be readily oxidized to N_2 , NO_2^- , and NO_3^- using a photocatalyst.^{14–17} The decomposition of aqueous NH_3 to H_2 and N_2 requires a standard Gibbs free energy change ΔG° of 18 kJ mol^{-1} (eqn (1)).¹⁸ This is significantly smaller than that required for the decomposition of H_2O to H_2 and O_2 (237 kJ mol^{-1} ; eqn (2)).



Because the photocatalytic oxidation of NH_3 and NH_4^+ is significantly more favorable than the oxidation of H_2O to O_2 ,¹⁸ it is possible to use NH_3 and NH_4^+ as electron donors in the photocatalytic conversion of CO_2 . Moreover, NH_3 has been considered for use as an efficient post-combustion CO_2 capture and storage (CCS) reagent because of its high absorption efficiency and loading capacity.¹⁹ The absorption and capture of CO_2 by an aqueous solution of NH_3 results in the formation of NH_4HCO_3 .²⁰ Other basic species, such as NaHCO_3 and KHCO_3 , have been used to increase the solubility of CO_2 in aqueous

^aDepartment of Molecular Engineering, Graduate School of Engineering, Kyoto University, Kyoto 615-8510, Japan. E-mail: teramura@moleng.kyoto-u.ac.jp; tanakat@moleng.kyoto-u.ac.jp

^bElements Strategy Initiative for Catalysts and Batteries, Kyoto University, Kyoto 615-8510, Japan

† Electronic supplementary information (ESI) available: Experimental details, calculations and characterizations. See DOI: 10.1039/c7sc01851g

solutions.^{21,22} Previous reports have suggested that dissolved CO₂, rather than bicarbonate (HCO₃[−]) or carbonate (CO₃^{2−}) ions, is the active species in the reduction of CO₂.^{23,24} Correspondingly, the conversion of CO₂ and/or the selectivity toward CO evolution have been significantly enhanced by the presence of bases in both photocatalytic (PC) and photoelectrochemical (PEC) cell systems.^{25,26} In the present study, we designed the use of NH₄HCO₃ for the efficient photocatalytic conversion of CO₂ to CO in H₂O.

Results and discussion

Flux-mediated crystal growth method shows the advantage of the synthetic control over particle sizes, morphologies, and surface features comparing with that of solid-state reaction method (SSR).²⁷ Modification of these features as a function of flux conditions have been reported to show significant enhancements in both water splitting and CO₂ photoreduction.^{11,27,28} Sr₂KTa₅O₁₅ has been reported to show good activity and selectivity toward CO evolution when used as a photocatalyst in the conversion of CO₂ by H₂O in our previous work.²⁹ In the present study, Sr₂KTa₅O₁₅ was fabricated by a modified flux method, using a mixture of NaCl and KCl as the flux. The resultant catalyst was confirmed to have tetragonal tungsten bronze (TTB) structure (Fig. S1A†), and its real chemical formula was determined to be Sr_{1.6}K_{0.35}Na_{1.45}Ta₅O₁₅ using ICP-OES. Its morphology was observed by SEM, and was found to consist of a mixture of nanorods and nanoparticles (Fig. S1B†).

Fig. 1 shows the time courses of the photocatalytic conversion of CO₂ in H₂O and aqueous solutions of NaHCO₃ and NH₄HCO₃. In pure H₂O, only 16.8 μmol of CO was evolved after 5 h of photoirradiation (Fig. 1A), and the main reduction product was H₂ (139.0 μmol). These results were consistent with previous reports.^{25,29} In this system, overall water splitting proceeded more readily than CO₂ reduction, resulting in the generation of H₂ as the major product, rather than CO. The amount of CO evolved in 0.1 M aqueous NaHCO₃ solution after 5 h of photoirradiation (448.7 μmol) was 26.7 times higher than that evolved in pure H₂O (Fig. 1B). However, the formation of H₂ (94.7 μmol) was not significantly affected by NaHCO₃. Thus,

NaHCO₃ greatly enhanced the conversion of CO₂ to CO without affecting the water splitting process.²⁵ In both pure H₂O and 0.1 M aqueous NaHCO₃, stoichiometric amounts of O₂ were evolved continuously during the reaction, implying that H₂O functioned as an electron donor in the reduction of CO₂. Moreover, the evolution of CO increased dramatically in 0.1 M aqueous NH₄HCO₃ solution; 1600 μmol (1.6 mmol) of CO was evolved after 5 h of photoirradiation (Fig. 1C). This is 94.2 times greater than the amount evolved in pure H₂O. The selectivity of the reaction toward CO evolution was calculated and the details were shown in ESI.† The selectivity toward CO evolution in 0.1 M aqueous NH₄HCO₃ (86.2%) was similar to that in aqueous NaHCO₃ (82.5%). The production of gaseous products was negligible in blank tests conducted without either a catalyst or photoirradiation (Fig. S2A and B†). Thus, both are necessary for the photocatalytic conversion of CO₂ to CO to proceed. Without Ag cocatalyst, H₂ was formed as main product (Fig. S2C†), both of N₂ and O₂ were detected as oxidation products, however, the amount of these gases was far beyond the stoichiometric amount. Tiny amount of CO was formed after 5 hour photoirradiation (14.9 μmol). Ag cocatalysts were important in photocatalytic conversion of CO₂ to CO, which is thought to be the active sites. H₂, CO, and N₂ were obtained without a continuous CO₂ flow (Fig. S2D†). However, H₂ was generated as a major product, suggesting a very low selectivity toward CO evolution (less than 30%). This suggested that CO₂ presence significantly increases the selectivity of the photocatalytic conversion of CO₂ toward CO evolution in NH₄HCO₃ solution. NH₄HCO₃ can be formed directly by the absorption of CO₂ in an aqueous solution of NH₃; wherein H₂ and CO can be produced from CO₂ and NH₃ *via* artificial photosynthesis. Thus, our designed system can achieve carbon capture and utilization (CCU) in a single process.

N₂, rather than O₂, was generated as the oxidation product during photoirradiation in the presence of NH₄HCO₃ (Fig. 1C). This demonstrated that H₂O did not function as an electron donor in this system. Instead, NH₃ and/or NH₄⁺ functioned as electron donors, because the Δ*G*^o of NH₃(aq) oxidation (18 kJ mol^{−1}) is significantly lower than that of water oxidation (237 kJ mol^{−1}). Analysis of the liquid phase showed that neither NO₂[−]



Fig. 1 Time courses of CO (circle), O₂ (square), N₂ (lozenge), and H₂ (triangle) evolutions during the photocatalytic conversion of CO₂ over Ag-modified Sr_{1.6}K_{0.35}Na_{1.45}Ta₅O₁₅. Amount of catalyst: 0.5 g; cocatalyst loading: 1.0 wt% Ag; light source: 400 W high-pressure Hg lamp; water volume: 1.0 L; CO₂ flow rate: 30 mL min^{−1}; additive: (A) none, (B) 0.1 M NaHCO₃, or (C) 0.1 M NH₄HCO₃.



nor NO_3^- were present during photoirradiation (Fig. S3†). Other gaseous NO_x products, such as N_2O and NO , were not detected by gas chromatography (GC). These results indicated that NH_3 and/or NH_4^+ were oxidized only to N_2 in this photocatalytic system. Hence, by using NH_4HCO_3 , we succeeded in controlling the oxidation product, in addition to enhancing the conversion of CO_2 .

The ratio of electrons to holes consumed in the photocatalytic conversion of CO_2 was calculated to be 2.0 after 1 h of photoirradiation (Fig. S4†). Given that the total number of electrons generated must be the same as the number of holes, this ratio indicates that significantly more electrons were consumed than holes in the initial stages of photoirradiation. We noted that the state of Ag was changed from metallic to Ag^+ on the surface of catalyst measured by XPS (Fig. S5†), however, it might be not the main reason for the excess of electron consumption. We calculated that if all Ag^0 was changed to Ag^+ in the first hour, the consumed holes were still only 469 μmol , which was much less than the consumed electrons (770 μmol). NH_4^+ can be reduced to NH_3 and H_2 by photogenerated electrons. Hydrazine (N_2H_4) has been determined to be an intermediate species in the photocatalytic decomposition of NH_3 and/or NH_4^+ to H_2 and N_2 using Pt/TiO_2 .¹⁴ Stoichiometric amounts of products, including H_2 and N_2 , were not obtained in the initial stages of photoirradiation due to the formation of hydrazine. In our system, it is also possible to form hydrazine at the beginning, however, hydrazine is reported to be reacted with CO_2 to form zwitterionic intermediate and carbamate-type species,³⁰ which made the detection of intermediate oxidation species much more difficult. Nevertheless, stoichiometric amounts of products were obtained after 2 h of photoirradiation (Fig. S4†), indicating that the total decomposition of NH_3 and/or NH_4^+ occurred sooner.

The above results demonstrate that the highly efficient photocatalytic conversion of CO_2 to CO was achieved in our system. The stoichiometric amounts of H_2 , N_2 and CO generated indicated that NH_3 and/or NH_4^+ functioned as electron donors in the photocatalytic conversion of CO_2 . Significantly greater photocatalytic activity was obtained using NH_3 and/or NH_4^+ , compared to reactions using H_2O as an electron donor under the same conditions. NH_3 and/or NH_4^+ are suitable for use in practical applications because NH_3 is industrially produced in large quantities. Furthermore, in our photocatalytic system, NH_3 and/or NH_4^+ can be completely decomposed to N_2 , which is an inert and non-toxic gas.

Table 1 shows the effects of NH_4HCO_3 concentration on the photocatalytic conversion of CO_2 . In pure H_2O , overall water splitting proceeded as the dominant reaction. Hence, the evolution of CO was negligible (entry 1). When the photocatalytic reaction was carried out in 0.01 M aqueous NH_4HCO_3 the production of H_2 resulting from water splitting was dramatically suppressed (entry 2). Because the oxidation of NH_3 and/or NH_4^+ to N_2 proceeds more readily than the oxidation of H_2O to O_2 , the formation rate of O_2 in 0.01 M aqueous NH_4HCO_3 was less than half that in pure H_2O . Even low concentrations of NH_4HCO_3 (0.01 M) significantly increased the formation rate of CO , indicating that the presence of NH_4HCO_3

is vital to achieving high photocatalytic activity. NH_4HCO_3 can also be used to increase the pH of the reaction solution, to offset the decrease in pH caused by the dissolution of CO_2 . With CO_2 flowing, the pH of the reaction solution based on pure H_2O was 3.95, which increased to 5.88 with the addition of 0.01 M NH_4HCO_3 . Increasing the pH also increases the amount of CO_2 that can be dissolved in the reaction solution.³¹ Generally, the formation rate of CO increases with increasing pH, because the reaction rate largely depends on the concentration of substrate. Therefore, the addition of NH_4HCO_3 contributed to the efficient conversion of CO_2 and the good selectivity toward CO evolution. Increasing the concentration of NH_4HCO_3 from 0.01 M to 0.05 M completely suppressed the overall water splitting reaction, since only N_2 was generated as an oxidation product (entry 3). The formation rate of CO increased with the concentration of NH_4HCO_3 . Increasing the NH_4HCO_3 concentration from 0.1 M to 1.0 M increased the formation rate of CO to 550.7 $\mu\text{mol h}^{-1}$ except the selectivity toward CO evolution decreased slightly, from 86.1% to 65.5% (entry 4 to 7). As previously discussed, NH_4HCO_3 can be synthesized by flowing CO_2 through an aqueous solution of NH_3 . To determine whether NH_3 functions as an electron donor under a flow of CO_2 , we carried out the photocatalytic conversion of CO_2 in an aqueous solution of NH_3 (entry 8). The formation rate of CO was 547.2 $\mu\text{mol h}^{-1}$ in ca. 0.5 M aqueous NH_3 , indicating that NH_3 functions efficiently as an electron donor under these conditions. The ratio of photo-generated electrons to holes (e^-/h^+) was estimated to be around 1.0 in reactions with high concentrations of aqueous NH_4HCO_3 after 5 h of photoirradiation. This further supports the hypothesis that NH_3 and/or NH_4^+ function as effective electron donors during the photocatalytic conversion of CO_2 .

To confirm that CO evolution originated from CO_2 introduced in the gas phase, rather than from carbon contaminants, we conducted an isotopic labeling experiment. Fig. 2 shows mass spectra ($m/z = 28$ and 29) obtained during the photocatalytic conversion of $^{13}\text{CO}_2$ in 0.5 M aqueous NH_4HCO_3 over Ag-

Table 1 Photocatalytic conversion of CO_2 over Ag-modified $\text{Sr}_{1.6}\text{-K}_{0.35}\text{Na}_{1.45}\text{Ta}_5\text{O}_{15}$ with different additive concentrations. Amount of catalyst: 0.5 g; cocatalyst loading: 1.0 wt% Ag; light source: 400 W high-pressure Hg lamp; water volume: 1.0 L; CO_2 flow rate: 30 mL min^{-1}

Entry	$\text{NH}_4\text{HCO}_3^a/\text{M}$	Formation rate ^b / $\mu\text{mol h}^{-1}$				Select. ^c (%)	$e^-/h^+{}^d$
		H_2	O_2	N_2	CO		
1	0	35.9	16.3	Trace	3.6	9.2	1.21
2	0.01	16.9	7.0	12.3	54.5	76.3	1.17
3	0.05	23.8	Trace	42.3	146.7	86.1	1.34
4	0.1	48.4	Trace	94.3	270.4	84.8	1.13
5	0.5	119.8	Trace	193.6	512.9	81.1	1.09
6	0.8	175.4	Trace	213.3	520.0	74.8	1.09
7	1.0	290.1	Trace	258.1	550.7	65.5	1.09
8 ^e	—	235.0	Trace	244.9	547.2	70.0	1.06

^a Additive concentration used for CO_2 conversion. ^b Formation rate after 5 h of irradiation. ^c Selectivity toward CO evolution. ^d Ratio of consumed electrons to holes after 5 h of irradiation. ^e 0.5 M aqueous NH_3 solution was used as the additive, instead of NH_4HCO_3 .





Fig. 2 Gas chromatogram and mass spectra ($m/z = 28$ and 29) obtained during the photocatalytic conversion of $^{13}\text{CO}_2$ using Ag-modified $\text{Sr}_{1.6}\text{K}_{0.35}\text{Na}_{1.45}\text{Ta}_5\text{O}_{15}$. Amount of catalyst: 0.5 g; cocatalyst loading: 5.0 wt% Ag; light source: 400 W high-pressure Hg lamp; water volume: 1.0 L; CO_2 flow rate: 30 mL min^{-1} ; additive: 0.5 M NH_4HCO_3 .

modified $\text{Sr}_{1.6}\text{K}_{0.35}\text{Na}_{1.45}\text{Ta}_5\text{O}_{15}$ after 0.5 h of photoirradiation. Gaseous samples were introduced into a mass spectrometer (MS) after separation by thermal conductivity detector-gas chromatography (TCD-GC). CO was observed in both the gas chromatogram and the mass spectra. The peak positions in the mass spectra were consistent with those in the chromatogram. The major product was ^{13}CO , rather than ^{12}CO . The presence of a small amount of ^{12}CO may be due to the direct decomposition of NH_4HCO_3 since the decomposition of NH_4HCO_3 was observed in samples without a CO_2 flow (Fig. S2D†). The amount of ^{13}CO estimated by mass spectrometry was approximately equal to the amount of CO determined using a flame ionization detector (FID-GC) (Fig. S6†). These results demonstrate that CO was predominantly generated from CO_2 introduced in the gas phase, rather than from other carbon resources.

The recycle test was also performed to confirm the stability and durability of our catalyst and system using the $\text{Sr}_{1.6}\text{K}_{0.35}\text{Na}_{1.45}\text{Ta}_5\text{O}_{15}$ photocatalyst repeatedly for three times under the same conditions (Fig. S7†). In the second cycle, there is a slight loss by *ca.* 10% of CO evolution activity during 5 h photoirradiation as compared to the first run, however, the evolution of H_2 showed no obvious changes. The slight loss of activity should be due to the change of Ag cocatalyst (Fig. S5†).²⁹ The photocatalytic activity of CO, N_2 , and H_2 were stabilized at *ca.* 0.5, 0.19 and 0.07 mmol h^{-1} , respectively, during the second and third runs. The structure of catalyst itself was stable during the three cycles (Fig. S8†). These results suggested that the photocatalyst and the system exhibit favorable stability to form CO, N_2 , and H_2 during the photocatalytic conversion of CO_2 .

Table 2 Photocatalytic conversion of CO_2 over Ag-modified catalysts in aqueous NH_4HCO_3 solution. Amount of catalyst: 0.5 g; cocatalyst loading: 5.0 wt% Ag; light source: 400 W high-pressure Hg lamp; water volume: 0.95 L; CO_2 flow rate: 30 mL min^{-1} ; additive: 0.5 M NH_4HCO_3

Entry	Catalyst	Formation rate ^a / $\mu\text{mol h}^{-1}$			Selec. ^b (%)	e^-/h^+ ^c
		H_2	N_2	CO		
1	$\text{ZnGa}_2\text{O}_4/\text{Ga}_2\text{O}_3$	125.2	191.4	532.0	80.9	1.14
2	ZnGa_2O_4	39.4	94.2	305.4	88.6	1.22
3	$\text{La}_2\text{Ti}_2\text{O}_7$	5.9	17.4	41.6	87.6	0.91
4	$\text{SrO}/\text{Ta}_2\text{O}_5$	2.71	11.5	42.9	94.1	1.32

^a Formation rate after 5 h of irradiation. O_2 was not detected in any of the samples. ^b Selectivity toward CO evolution. ^c Ratio of consumed electrons to holes after 5 h of irradiation.

To confirm the versatility of NH_4HCO_3 as a general electron donor in photocatalytic reactions, we carried out the photocatalytic conversion of CO_2 in aqueous NH_4HCO_3 solution over 4 types of photocatalysts. All these photocatalysts have been already reported to show good activity and high selectivity toward CO evolution in the photocatalytic conversion of CO_2 using H_2O as an electron donor.^{25,32–34} As shown in Table 2, all the photocatalysts showed good activity for conversion of CO_2 and high selectivity toward CO evolution. The activities of the photocatalysts were significantly increased in aqueous NH_4HCO_3 solution, compared with their reported activities in pure H_2O or aqueous NaHCO_3 .^{32–34} N_2 was detected as the only oxidation product and the e^-/h^+ ratio was approximately equal to 1.0. These results indicated that NH_3 and/or NH_4^+ was easily decomposed to N_2 gas by the photocatalysts tested.

Conclusions

We designed a highly efficient process for the photocatalytic conversion of CO_2 to CO in aqueous NH_4HCO_3 solution. The stoichiometric formation of CO, H_2 , and N_2 indicated that NH_3 and/or NH_4^+ were consumed as electron donors, instead of H_2O . NH_4HCO_3 was determined to be an effective electron donor for the photocatalytic conversion of CO_2 , whereby CO_2 can be captured, stored, and efficiently converted into CO. This novel inorganic additive is suitable for use in carbon capture and utilization process. This new process is a promising way to control the conversion of CO_2 to CO and efficiently produce H_2 and CO.

Acknowledgements

This study was partially supported by a Grant-in-Aid for Scientific Research on Innovative Areas “All Nippon Artificial Photosynthesis Project for Living Earth” (No. 2406) from the Ministry of Education, Culture, Sports, Science, and Technology (MEXT) of Japan, the Precursory Research for Embryonic Science and Technology (PRESTO), supported by the Japan Science and Technology Agency (JST), and the Program for Elements Strategy Initiative for Catalysts & Batteries (ESICB),



commissioned by the MEXT of Japan. Zeai Huang thanks the State Scholarship of China Scholarship Council, affiliated with the Ministry of Education of the P. R. China.

Notes and references

- 1 S. N. Habisreutinger, L. Schmidt-Mende and J. K. Stolarczyk, *Angew. Chem., Int. Ed.*, 2013, **52**, 7372–7408.
- 2 G. Centi, E. A. Quadrelli and S. Perathoner, *Energy Environ. Sci.*, 2013, **6**, 1711–1731.
- 3 K. Teramura, S. Iguchi, Y. Mizuno, T. Shishido and T. Tanaka, *Angew. Chem.*, 2012, **124**, 8132–8135.
- 4 R. Kuriki, K. Sekizawa, O. Ishitani and K. Maeda, *Angew. Chem., Int. Ed.*, 2015, **54**, 2406–2409.
- 5 R. Kuriki, H. Matsunaga, T. Nakashima, K. Wada, A. Yamakata, O. Ishitani and K. Maeda, *J. Am. Chem. Soc.*, 2016, **138**, 5159–5170.
- 6 S. Navalón, A. Dhakshinamoorthy, M. Álvaro and H. Garcia, *ChemSusChem*, 2013, **6**, 562–577.
- 7 X. Chang, T. Wang and J. Gong, *Energy Environ. Sci.*, 2016, **9**, 2177–2196.
- 8 G. Liu, S. Xie, Q. Zhang, Z. Tian and Y. Wang, *Chem. Commun.*, 2015, **51**, 13654–13657.
- 9 K. Iizuka, T. Wato, Y. Miseki, K. Saito and A. Kudo, *J. Am. Chem. Soc.*, 2011, **133**, 20863–20868.
- 10 M. Yamamoto, T. Yoshida, N. Yamamoto, T. Nomoto, Y. Yamamoto, S. Yagi and H. Yoshida, *J. Mater. Chem. A*, 2015, **3**, 16810–16816.
- 11 H. Yoshida, L. Zhang, M. Sato, T. Morikawa, T. Kajino, T. Sekito, S. Matsumoto and H. Hirata, *Catal. Today*, 2015, **251**, 132–139.
- 12 H. Nakanishi, K. Iizuka, T. Takayama, A. Iwase and A. Kudo, *ChemSusChem*, 2017, **10**, 112–118.
- 13 K. Hara, A. Kudo, T. Sakata and M. Watanabe, *J. Electrochem. Soc.*, 1995, **142**, L57–L59.
- 14 H. Yuzawa, T. Mori, H. Itoh and H. Yoshida, *J. Phys. Chem. C*, 2012, **116**, 4126–4136.
- 15 H. Wang, Y. Su, H. Zhao, H. Yu, S. Chen, Y. Zhang and X. Quan, *Environ. Sci. Technol.*, 2014, **48**, 11984–11990.
- 16 X. Zhu, S. R. Castleberry, M. A. Nanny and E. C. Butler, *Environ. Sci. Technol.*, 2005, **39**, 3784–3791.
- 17 S. Yamazoe, Y. Hitomi, T. Shishido and T. Tanaka, *Appl. Catal., B*, 2008, **82**, 67–76.
- 18 H. Kominami, H. Nishimune, Y. Ohta, Y. Arakawa and T. Inaba, *Appl. Catal., B*, 2012, **111**, 297–302.
- 19 B. T. Zhao, Y. X. Su, W. W. Tao, L. L. Li and Y. C. Peng, *Int. J. Greenhouse Gas Control*, 2012, **9**, 355–371.
- 20 X. Wang, W. Conway, D. Fernandes, G. Lawrance, R. Burns, G. Puxty and M. Maeder, *J. Phys. Chem. A*, 2011, **115**, 6405–6412.
- 21 S. F. Shen, Y. N. Yang and S. F. Ren, *Fluid Phase Equilib.*, 2014, **367**, 38–44.
- 22 H. Zhong, K. Fujii, Y. Nakano and F. Jin, *J. Phys. Chem. C*, 2015, **119**, 55–61.
- 23 B. Kumar, M. Llorente, J. Froehlich, T. Dang, A. Sathrum and C. P. Kubiak, *Annu. Rev. Phys. Chem.*, 2012, **63**, 541–569.
- 24 Y. Hori, A. Murata and R. Takahashi, *J. Chem. Soc., Faraday Trans. 1*, 1989, **85**, 2309–2326.
- 25 K. Teramura, Z. Wang, S. Hosokawa, Y. Sakata and T. Tanaka, *Chem.–Eur. J.*, 2014, **20**, 9906–9909.
- 26 E. E. Barton, D. M. Rampulla and A. B. Bocarsly, *J. Am. Chem. Soc.*, 2008, **130**, 6342–6344.
- 27 J. Boltersdorf, N. King and P. A. Maggard, *CrystEngComm*, 2015, **17**, 2225–2241.
- 28 Y. Ham, T. Hisatomi, Y. Goto, Y. Moriya, Y. Sakata, A. Yamakata, J. Kubota and K. Domen, *J. Mater. Chem. A*, 2016, **4**, 3027–3033.
- 29 Z. Huang, K. Teramura, S. Hosokawa and T. Tanaka, *Appl. Catal., B*, 2016, **199**, 272–281.
- 30 K. H. Lee, B. Lee, J. H. Lee, J. K. You, K. T. Park, I. H. Baek and N. H. Hur, *Int. J. Greenhouse Gas Control*, 2014, **29**, 256–262.
- 31 K. Teramura, K. Hori, Y. Terao, Z. Huang, S. Iguchi, Z. Wang, H. Asakura, S. Hosokawa and T. Tanaka, *J. Phys. Chem. C*, 2017, **121**, 8711–8721.
- 32 Z. Wang, K. Teramura, S. Hosokawa and T. Tanaka, *J. Mater. Chem. A*, 2015, **3**, 11313–11319.
- 33 Z. Wang, K. Teramura, S. Hosokawa and T. Tanaka, *Appl. Catal., B*, 2015, **163**, 241–247.
- 34 K. Teramura, H. Tatsumi, Z. Wang, S. Hosokawa and T. Tanaka, *Bull. Chem. Soc. Jpn.*, 2015, **88**, 431–437.

